



**HAL**  
open science

## Influence of non-ideal clamping in microcantilever resonant frequency estimation

Ludivine Fadel-Taris, Cédric Ayela, Isabelle Dufour, Fabien Josse, Stephen Heinrich, Daisuke Saya, Oliver Brand

► **To cite this version:**

Ludivine Fadel-Taris, Cédric Ayela, Isabelle Dufour, Fabien Josse, Stephen Heinrich, et al.. Influence of non-ideal clamping in microcantilever resonant frequency estimation. 2011 IEEE International Frequency Control Symposium, 2011, San Francisco, United States. 5 p., 10.1109/FCS.2011.5977310 . hal-00564420

**HAL Id: hal-00564420**

**<https://hal.science/hal-00564420v1>**

Submitted on 28 Apr 2022

**HAL** is a multi-disciplinary open access archive for the deposit and dissemination of scientific research documents, whether they are published or not. The documents may come from teaching and research institutions in France or abroad, or from public or private research centers.

L'archive ouverte pluridisciplinaire **HAL**, est destinée au dépôt et à la diffusion de documents scientifiques de niveau recherche, publiés ou non, émanant des établissements d'enseignement et de recherche français ou étrangers, des laboratoires publics ou privés.

# Influence of non-ideal clamping in microcantilever resonant frequency estimation

L. Fadel-Taris, C. Ayela, I. Dufour  
 Université de Bordeaux, CNRS, IMS Laboratory  
 Talence, France  
[cedric.ayela@ims-bordeaux.fr](mailto:cedric.ayela@ims-bordeaux.fr)

D.Saya  
 LAAS-CNRS  
 Toulouse, France

F. Josse, S.M. Heinrich  
 Marquette University  
 Milwaukee, USA  
[stephen.heinrich@marquette.edu](mailto:stephen.heinrich@marquette.edu)

O. Brand  
 School of Electrical and Computer Engineering  
 Georgia Institute of Technology  
 Atlanta, USA

**Among the most promising sensing platforms are resonating microcantilevers due to their high sensitivity and wide application range. A key parameter of the device implementation is the predicted value of the resonant frequency that depends on the modeling and considerations of relevant physical phenomena. In fact, the estimation based on the conventional, perfectly clamped, Bernoulli-Euler cantilever beam does not lead to satisfactory accuracy in certain cases. Hence this work investigates two system characteristics that may affect the resonant frequency (a support effect and a so-called rim effect) and provides solutions for a straightforward estimation of rim dimension using resonance behavior of the cantilevers.**

## I. INTRODUCTION

Among the most promising sensing platforms are resonating microcantilevers due to their high sensitivity and wide application range for chemical sensing. A key parameter of the device implementation is the predicted value of the resonant frequency, which depends on the modeling and considerations of relevant physical phenomena. The classical expression used for the first transverse resonant frequency of a clamped-free microcantilever is obtained from the solution of the Euler-Bernoulli equation for a cantilever in vacuum [1]:

$$f_0 = \frac{\lambda_0^2 h}{2\pi L^2} \sqrt{\frac{E}{12\rho}} \quad (1)$$

With  $\lambda_0 = 1.875$ ,  $h$  the cantilever thickness,  $L$  the cantilever length,  $E$  and  $\rho$  the Young's modulus and mass density of the cantilever material, respectively. In fact, when compared to measurement, this equation does not lead to a satisfactorily accurate result in certain cases. For example, in the case of a silicon cantilever  $504\mu\text{m} \times 100\mu\text{m} \times 20\mu\text{m}$ , with the cantilever length parallel to the  $\langle 110 \rangle$  direction of the silicon  $\langle 100 \rangle$  wafer, the measured resonant frequency is  $94.4\text{kHz}$ ,

whereas the theoretical resonant frequency using (1) with the mechanical properties of silicon in this configuration ( $E = 169\text{GPa}$ ,  $\rho = 2330\text{kg/m}^3$ ) leads to  $108.3\text{kHz}$  (15% higher than the measured value). Assuming that the geometry of the cantilever and the boundary conditions are not the error sources, two possible reasons for the difference between the theoretical and measured resonant frequency may be envisioned: the presence of the air as the surrounding medium instead of vacuum and the shear strain which is not considered in the Euler-Bernoulli equation.

The presence of the surrounding medium can be taken into account by considering the hydrodynamic force per unit length exerted by the air on the cantilever. This force per unit length is composed of both a viscous part proportional to the cantilever velocity (term noted  $g_1$ ) and an inertial part proportional to the cantilever acceleration (term noted  $g_2$ ) [2]. Equation 1 has to be modified by taking into account this force, resulting in [3]:

$$f_r = f_0 \frac{\sqrt{1 - \frac{1}{2Q^2}}}{\sqrt{1 + \frac{g_2}{m_L}}}; \quad (2)$$

with  $m_L$  the cantilever mass per unit length and  $Q$  the quality factor defined by [3]:

$$Q = \frac{2\pi\sqrt{1 + g_2/m_L}}{g_1/m_L} f_0 \quad (3)$$

Using these equations and appropriate values for  $g_1$  and  $g_2$  [3], the resonant frequency in air ( $107.1\text{kHz}$ ) is smaller than in vacuum but the difference is not sufficient to predict the measured resonant frequency.

The Timoshenko beam theory [4] allows taking into account the shear strain and rotational inertia effects which are not considered in Eq.1. Again, these effects are not significant enough to account for the decrease in the resonant frequency that is seen in the measurements.

This leads one to consider that frequency discrepancy may be due to variations in the geometry and/or the boundary conditions. As detailed in the following section, the fabrication process may result in cantilever and support geometry that is not exactly the same as the one considered in the solution of the Euler-Bernoulli equation for a perfectly clamped cantilever. In this context, the work presented in this paper investigates two system characteristics that may affect the resonance mode and associated resonant frequency: the elasticity of the support which doesn't clamp ideally the supported end of the cantilever and the effect of a fabrication-induced silicon undercut that can occur during the release process of the suspended structures by Deep Reactive Ion Etching (DRIE).

## II. MOTIVATION

Classically, silicon microcantilevers are fabricated by means of silicon standard micromachining techniques using a process in which release of the structures is based on a backside etching of the wafer. For this, Silicon-On-Insulator (SOI) substrates are commonly used in which a thin silicon dioxide layer insulates the backside silicon etching, either using a wet or dry etching process. This results in free-standing microcantilevers clamped on a thick silicon support. An example of silicon microcantilevers with silicon support is shown on figure 1. From this figure, a free-standing microcantilever is clearly visible, but a silicon undercut at the clamped end of the cantilever is also visible, due to silicon over-etching during backside etching. (In the present case, silicon backside etching is provided by means of DRIE.) A consequence is a loss of rigidity at the supported end of the cantilever, resulting in possible mechanical deformation of the undercut part, which in this paper will be referred to as the "rim" (Fig. 1).

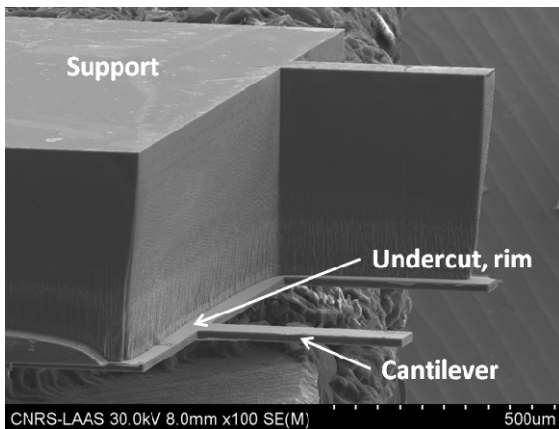


Figure 1: SEM picture of a microcantilever released by DRIE on a SOI wafer. Visualization of the silicon support and over-etching (rim).

In the present analysis, two origins in the discrepancy between theoretical and experimental values of resonant frequency of microcantilevers have been identified: a support compliance effect and an effect due to silicon over-etching, i.e., the so-called rim effect. First, the impact of both effects on the resonant frequency has been simulated using COMSOL. For this, a cantilever with ideal clamping (no rim, rigid support) has been simulated and the results compared to resonant frequency predictions for the case in which the structure is supported by an elastic rim attached to a rigid support block (rim length = 35µm in the simulation). Then, the impact of both effects (combined) has been simulated. The comparison of results is indicated in the schematic diagram of figure 2. This figure shows that the combined effect of rim and support is significant: the simulated resonant frequency is 11.3% lower than for the ideally-clamped cantilever. The results also show that the rim effect dominates the support compliance effect since a decrease of resonant frequency of 10% is due to the rim and thus, 1.3% due to the support elasticity. In this context, the systematic and direct (i.e. without the need of a backside observation of the chip) estimation of the rim length is of particular interest. This will lead to an appropriate use of the structures in the broad range of applications covered by resonant microcantilevers. The objective for the present work is thus to develop a method for using the resonance behavior of microcantilevers to determine the rim length at the supported end of the structures. Future work will include the development of an analytical expression for the cantilever resonant frequency which takes into account the rim effect.

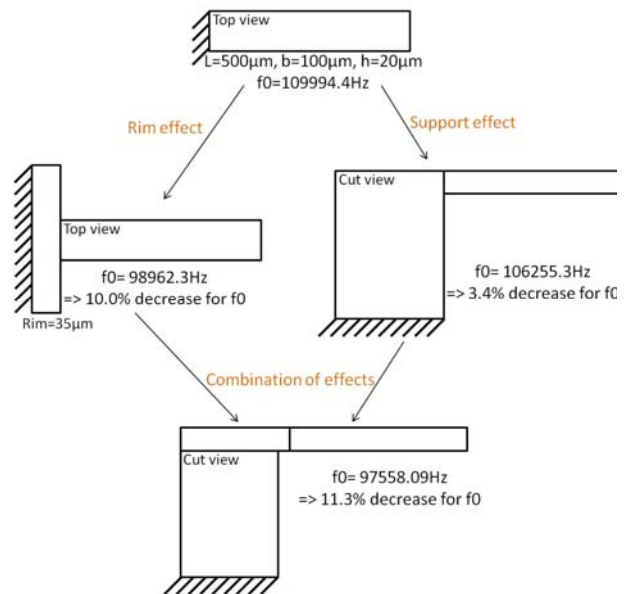


Figure 2: Microcantilever geometries and resonant frequencies obtained by COMSOL simulation in the case of a) ideal clamping, b) rim effect, c) support effect, d) combination of effects.

### III. EXPERIMENTAL SECTION

#### A. Cantilever fabrication

Free-standing microcantilevers have been fabricated by standard micromachining techniques. Cantilevers are rectangular shaped with a length of 500 $\mu\text{m}$  and a width of 100 $\mu\text{m}$ . Each cantilever can be actuated individually by means of a Laplace force by incorporating both a patterned gold layer allowing a local current flow and an external magnet.

The main steps of the fabrication process are as follows. The starting substrate is a 100 mm-diameter, <100>, N-type Silicon-On-Insulator (SOI) wafer, with a 1  $\mu\text{m}$ -thick buried oxide and a 20  $\mu\text{m}$ -thick top silicon layer (resistivity of 4-6  $\Omega\cdot\text{cm}$ ). A first step consisted in the deposition of 300 nm of Plasma Enhanced Chemical Vapor Deposition (PECVD) silicon dioxide on the entire SOI wafer before the sputtering of Ti/Au (100 nm / 700 nm) for the electrode used for electromagnetic actuation. The film was lifted off with an AZ nLOF negative photoresist to define the electrode characterized by a width of 10  $\mu\text{m}$ . A passivation silicon oxide film (300 nm thick) was then deposited by PECVD. Contact pads were opened by wet etching of oxide using HF buffer. To finish, the microcantilever shapes were defined by a front Reactive Ion Etching of silicon, followed by vertical sidewalls etching on the backside of the SOI wafer using the Deep Reactive Ion Etching technique to release the structures. The 1  $\mu\text{m}$ -thick  $\text{SiO}_2$  acts as an etch stop layer for the dry silicon etching. This layer was then removed by Reactive Ion Etching. The cantilever chips were then mounted on a PCB by gluing the silicon support (figure 1) with epoxy glue. Wire bonding ensures communication between the chips and the PCB.

Figure 3 shows a close-up view of one cantilever obtained by dual-beam optical interferometry (Veeco NT9080). As shown in this figure, the rectangular geometry of the cantilever is clearly defined with respect to the design, as is the gold electrode used for integrated actuation. Also, as shown in figure 1, the release of the cantilever is clearly visible.

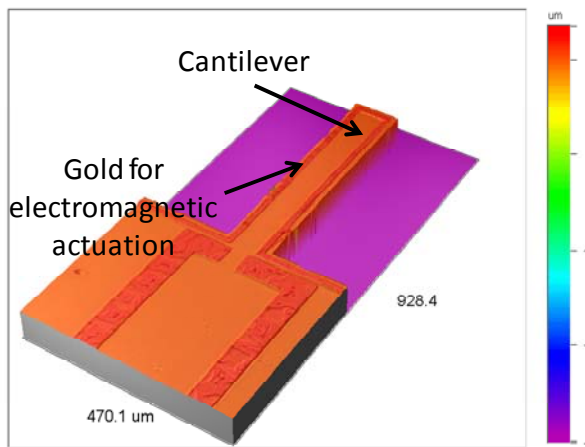


Figure 3: Geometry of the chip obtained by optical profilometry.

#### B. Rim pre-estimation by means of optical profiler

Prior to the development of methods for estimating the rim length using the resonant behavior of microcantilevers, the value of rim dimension is estimated by means of a dual-beam interferometry profiler. This optical tool was found to be the best compromise to achieve a balance of simplicity, accuracy and minimal time consumption. Concerning the measurement set-up, the cantilever chips were placed vertically under the objective of the profiler, so that the sidewall etching profile of the backside of the SOI wafer could be studied. An example of a profile acquired is shown in figure 4. From this figure, one sees that the verticality of the sidewall is not perfect, and the silicon over-etching is clearly visible. An undercut below the top silicon layer is evident, from which the rim length may be determined. For the different chips tested, the values of rim length that were measured are summarized in table 1. From this table, it can be seen that the rim lengths range from 15 to 35  $\mu\text{m}$ . The values obtained are consistent with the position of the chips on the wafer, since silicon over-etching decreases as one moves from the center to the periphery of the SOI substrate. (Chip A7 is at the periphery of the wafer while chips A100 and A102 are close to the center of the wafer.)

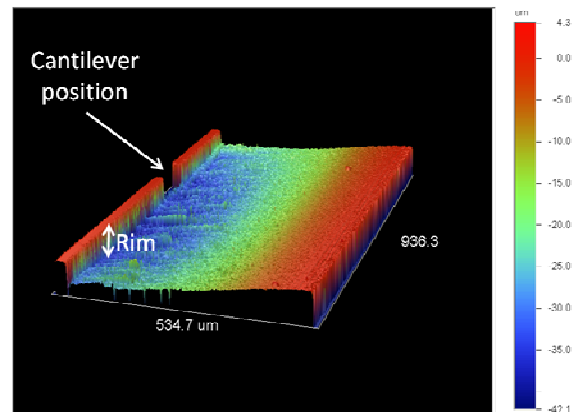


Figure 4: Sidewall etching profile measured by optical profilometry.

Table 1: Measured rim length (optical profiler).

Chip #	Measured rim length ( $\mu\text{m}$ )
A100	$34.7 \pm 0.8$
A102	$32.2 \pm 1.1$
A63	$35.5 \pm 1.4$
A7	$15.6 \pm 0.5$
A28	$26.7 \pm 3.2$

#### C. Rim length evaluation by means of cantilever resonance

In the present work, two methods based on the resonance behavior of microcantilevers are proposed to estimate the dimension of the rim, whose existence is primarily responsible for the inaccuracy of the conventional method for

estimating resonant frequency (1). The first method uses the value of the microcantilever resonant frequency, while the second one uses the deflection profile at resonance (i.e., the deformed beam shape) of the actual cantilever. For both methods, the first out-of-plane flexural resonant mode has been studied using a Polytec MSA-500 optical vibrometer. Actuation of the structures is performed by electromagnetic forces, while the deflection spectrum is acquired via the laser vibrometer, allowing a precise determination of resonant frequency (<1 Hz resolution). Also, the vibrometer system allows a specific meshing of the vibrating structure, so that a specific resonant mode shape can be studied quantitatively. Making use of this capability, the cantilever deflection profile at resonance has been acquired. A resulting ratio ( $R$ ) between deflection at the tip of the cantilever and the deflection at the clamped-end (i.e. at the beam/rim interface) has been calculated and compared to a calibration curve obtained via Finite Element Modeling (FEM) using COMSOL. For the resonant frequency method, a similar approach is proposed, but the values that are compared are those of resonant frequency. Using both methods, a rim value is determined by comparison between experimental data and the calibration curve.

#### IV. RESULTS AND DISCUSSION

By utilizing the resonance behavior of the cantilevers, the two methods outlined above have been employed to obtain estimates of the rim length, i.e., without the need of a backside (or side) observation of the chip. In the following, the details of the methods are given in addition to the results.

##### A. Resonant frequency method

The resonant frequency method is based on the fact that the resonant frequency clearly depends on the value of rim length because the presence of the rim induces a different mechanical rigidity at the supported end of the cantilever. Indeed, in figure 5 a calibration curve has been established via FEM where the simulated structure corresponds to the one designed, composed of bare silicon, PECVD SiO<sub>2</sub> and a gold electrode. As expected, the figure shows a decrease of resonant frequency when the rim length increases. This is mainly due to the loss of rigidity at the clamped-end of the cantilever when rim length increases. Also, in this figure has been plotted the value of resonant frequency measured on chips A7, A28, A100, A102. These chips, composed of cantilevers characterized by the same geometry, provide different resonant frequencies ranging from 92.5 kHz to 97.9 kHz. This indicates that different values of rim length are present for the tested chips. Indeed, by comparison between the calibration curve and the experimental values, rim length values ranging from 20.4 μm and 49 μm, have been determined. However, these values do not perfectly fit with values determined with the optical profiler, as shown in table 2. Note that in all cases, the proposed method overestimates the rim length, indicating that there exists other “softening effects” (e.g., support compliance) that the proposed method

does not include. A discrepancy between 14.4% and 30.8% in rim length estimation is observed for three of the four chips. The remaining chip (A28) has an 83.5% difference because the measured values of the frequency and rim length do not follow the trend of the other data (i.e., larger rim length should result in lower frequency). Thus, this data point may be suspect. Note that a slight loss of accuracy may result from other parameters not considered in the simulation, such as the exact thickness of the top silicon substrate or the thickness nonuniformity of the gold electrode. However, with the resonant frequency method, a simple and rapid estimation of rim has been demonstrated.

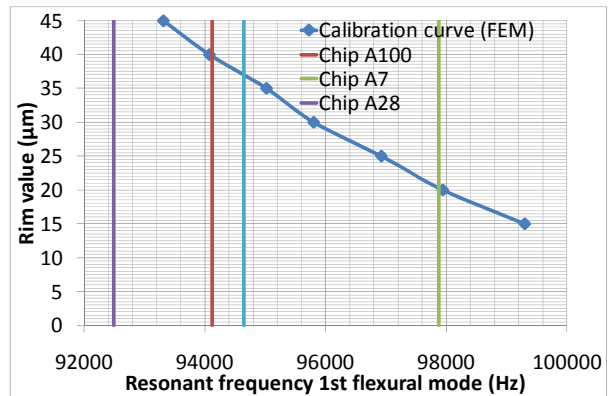


Figure 5: Determination of the rim length value using the resonant frequency measurement and the one obtained by COMSOL simulation.

Table 2: Comparison of the rim length estimation using resonant frequency measurement and the one obtained by optical profilometry.

	A100	A7	A28	A102
estimated rim length (optical profiler) (μm)	34.7	15.6	26.7	32.2
measured resonant frequency (Hz)	94116.2	97877.9	92492.1	94648.4
estimated rim length with resonant frequency (μm)	39.7	20.4	49	37

##### B. Resonant profile method

Since the rim influences the rigidity of the supported end of the cantilever, the large deflection obtained at resonance can induce a deformation in the rim structure and this deformation will, of course, depend on the rim length. With this in mind, the influence of the rim length on the deflection profile of the cantilever at resonance has been studied. In figure 6, the normalized resonant profiles of cantilevers for different values of rim length have been simulated by FEM. From this figure, the dependence of the resonant profile on rim length is evident, so that the ratio between tip deflection and deflection at the clamped-end (rim/cantilever interface) is proposed as a metric for rim length estimation. By comparison with the calibration curve obtained by FEM, values of rim length have been estimated, ranging from 18.3 μm to 26.7 μm as shown in table 3. With this method, it is observed that the rim length tends to be underestimated (in contrast to the frequency method) with the discrepancies being larger (between -30.7% and 17.3%) than those obtained

with the resonant frequency method (Again, the largest difference (-30.7%) corresponded to Chip A28). However, given the simplicity of the method and the possible error sources, mainly the difficulty in determining the exact position of the clamped-end of the cantilever for the determination of the deflection ratio, the values of rim length obtained give an approximate estimation of this important parameter.

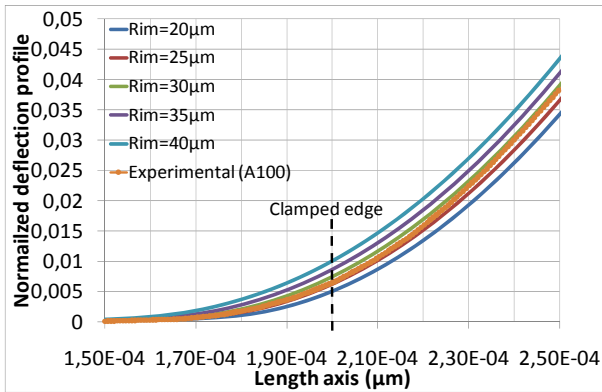


Figure 6: Deflection profile at resonance obtained for different values of rim length (COMSOL simulations).

Table 3: Comparison of the rim length estimation using the resonant profile method and the one measured by the optical profiler

	A100	A7	A28	A102
estimated rim length (optical profiler) ( $\mu\text{m}$ )	34.7	15.6	26.7	32.2
measured deflection ratio ( $w_{\text{tip}}/w_{\text{clamp}}$ )	151.24	220.87	213.2	176.6
estimated rim length with ratio ( $\mu\text{m}$ )	26.7	18.3	18.5	22.7

### C. Summary

The values of rim provided by optical profilometry (reference method) and the ones obtained with the alternative methods proposed for the four tested chips are summarized in figure 7. From this figure, it can be seen that the resonant frequency method tends to overestimate the rim length, while the resonant profile method tends to underestimate it (the exception being chip A7). Thus, by combination of both methods, a rim length range for each chip can be determined, while the average value gives an approximate value of rim length with a discrepancy magnitude as low as  $\sim 4\%$ , as obtained for the chip A100. These results are encouraging in that they provide some motivation for (a) further development of a combined method based on the resonant frequency and resonant profile methods, and (b) development of analytical models that show how various system parameters, including rim length, influence the resonant

behavior of a microcantilever/rim system. We envision the successful development of these types of models as being of paramount importance when using single or multiple (coupled) cantilever devices in sensing applications.

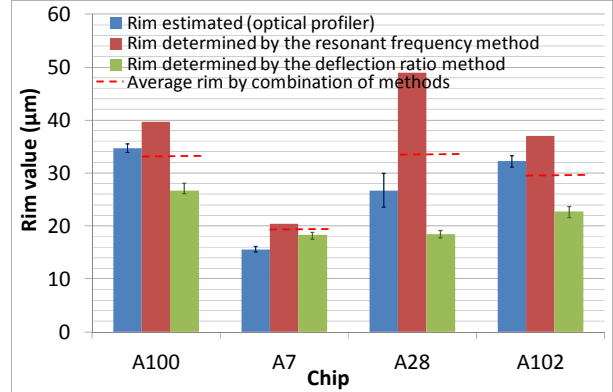


Figure 7: Summary of rim length estimation for the different methods investigated.

## V. CONCLUSION

In the present work, two straightforward methods based on resonance behavior of microcantilevers have been proposed and evaluated for the systematic determination of rim length due to silicon over-etching that can occur during DRIE. Using both the cantilever's observed resonant frequency and its deflection profile at resonance, the rim length was determined via comparisons with calibration curves obtained via FEM simulations. By combining both methods, good estimates of the rim length value have been achieved. However, due to the time-consuming nature of performing the requisite FEM simulations, the development of analytical solutions to the problem is desirable. Such analytical models are now under development, so that a better understanding of the complex interplay of system parameters may be obtained for resonating microcantilevers having non-standard support conditions.

- [1] R. D. Blevins, Formulas for natural frequency and mode shape, Ed. Van Nostrand Reinhold Company, New-York, ISBN 0-442-20710-7, 1979.
- [2] L D Landau, E M Lifshitz, A Course in Theoretical Physics - Fluid Mechanics, Pergamon Press Ltd., Vol. 6, 1987.
- [3] I. Dufour, S. Heinrich, F. Josse, "Theoretical analysis of strong-axis bending mode vibrations for resonant microcantilever (bio)chemical sensors in gas or liquid phase", Journal of MicroElectroMechanical Systems (IEEE/ASME Publication), Vol. 16, 2007, pp. 44-49.
- [4] Timoshenko et D. H. Young, Advanced Dynamics, McGraw-Hill Book Co., 1948